Effect of electrons produced by ionization on calculated electron-energy distributions

S. Yoshida* and A. V. Phelps†
Joint Institute for Laboratory Astrophysics, National Bureau of Standards and University of Colorado, Boulder, Colorado 80309

L. C. Pitchford
Sandia National Laboratory, Albuquerque, New Mexico 87185
(Received 9 November 1982)

The effects of the form of the distribution in energy of the electrons produced by ionization on electron-energy distributions and transport coefficients are investigated theoretically at high values of the ratio of the electric field to gas density, E/n. The calculations are carried out for N_2 at E/n from 100×10^{-21} to 3000×10^{-21} V m^2 using previously determined electron-collision cross sections and secondary-electron energy distributions. As the energy of the secondary electrons and the energy lost by the higher-energy, scattered electrons is increased, the relative numbers of electrons at very low energies and at high energies in the calculated steady-state distributions decreases. These changes are accompanied by decreases in the calculated ionization coefficients, drift velocities, and mean energies and by an increase in the characteristic energy. A simplified secondary-electron energy distribution is proposed which gives distribution functions and transport coefficients in satisfactory agreement with the those obtained using the published experimental distributions.

I. INTRODUCTION

The effect of the secondary electrons produced by electron impact ionization of atoms or molecules on electron transport and reaction rate coefficients is important at high values of the ratio of the electric field to the gas density, E/n. Recently, Brunet and Vincent[1] have investigated this problem theoretically for H_2 and N_2 taking into account the energy distribution of the secondary electrons measured by Opal, Peterson, and Beaty.[2] These calculations are an extension of calculations in which the distribution in energy of the electrons resulting from ionization has been approximated by δ functions[3–8] or by a uniform distribution.[9] In this paper we compare the electron-energy distributions, ionization coefficients, and transport coefficients obtained by solving the Boltzmann equation using the experimental secondary-electron distribution and various approximate energy distributions in common use. In addition, we introduce an empirical approximate secondary-energy distribution which yields results in agreement with results obtained with experimental distributions but which is much simpler to use. We will show that this simple approximate formula for the secondary-electron energy distribution is satisfactory for most solutions of the electron Boltzmann equation. The completion of a similar study utilizing Monte Carlo techniques has been reported by Kunhardt and Tzeng.[10]

Most calculations of electron-energy distributions make use of the two-term spherical harmonic expansion, i.e., the Lorentz approximation, to represent the angular dependence of the electron distribution in velocity space.[3,4] This approximation was used by Brunet and Vincent. A number of investigators[9–14] have found that the convergence of the coefficients of the spherical harmonics is slow at high E/n and have questioned the validity of the two-term approximation. However, several authors[14,15] find that ionization coefficients calculated using the two-term approximation agree well with coefficients calculated using more accurate calculations of the angular dependence of the electron-energy distribution. We therefore have carried out most of this investigation using modifications of a computer program[16] based on the conventional two-term approximation. Here the term "conventional" is taken to mean a steady-state solution in which inelastic collisions are omitted from the equation used to obtain the dipole coefficient of the anisotropic portion of the electron-energy distribution. The cross sections used are a recent set developed[15] for N_2 from electron transport and scattering data.

Rather than solve the spatially dependent, steady-state form of the Boltzmann equation considered by Brunet and Vincent, we will consider the solution appropriate to a spatially independent electron density which is increasing exponentially with time. We have considered this form of the problem in order to facilitate comparison with solutions of the Boltzmann equation given by the first term of the density gradient expansion as applied to N_2 by Pitchford and Phelps.[17] These approximations mean that our results do not include the effects of spatial gradients considered in several recent publications.[14,15] The kinetics of the ionization process and the electron Boltzmann equation are discussed in Sec. II. The results of the calculations are presented and discussed in Sec. III.

II. THEORETICAL FORMULATION

This section contains a review of the kinetics of electron impact ionization as required for application to the Boltzmann equation for electrons. We then discuss the form of the Boltzmann equation used in this investigation.

A. Ionization kinetics

Holstein[3] shows that the contribution of collisional ionization to the rate of increase of the electron-energy distribution $f(\epsilon)$ for energies between ϵ and $\epsilon+d\epsilon$ is given by the expression

$$\left[\frac{\partial f(\epsilon)}{\partial t}\right]_{\text{ion}} = \frac{vn}{\epsilon}\int_{2\epsilon+u_i}^{\infty} u q^i_{\text{sec}}(u,\epsilon) f(u)\,du + \frac{vn}{\epsilon}\int_{\epsilon+u_i}^{2\epsilon+u_i} u q^i_{\text{sca}}(u,\epsilon) f(u)\,du - vnQ_i(\epsilon) f(\epsilon)\,, \tag{1}$$

where $q^i_{\text{sec}}(u,\epsilon)$ is the differential ionization cross section for the process in which a primary electron of energy u produces a "secondary" electron of energy ϵ, $q^i_{\text{sca}}(u,\epsilon)$ is the differential cross section for the production of a "scattered" electron of energy ϵ by a primary electron of energy u, n is the density of gas molecules and u_i is the ionization potential. Here v is the speed of an electron with energy ϵ. The first term of Eq. (1) accounts for all of the secondary electrons which reenter the distribution with energies between ϵ and $\epsilon+d\epsilon$ as the result of ionizing collisions by primary electrons with energies between $u=2\epsilon+u_i$ and ∞. Similarly, the second term accounts for scattered primary electrons which reenter the distribution at an energy ϵ as the result of ionizing collisions by electrons with energies between $u=\epsilon+u_i$ and $u=2\epsilon+u_i$. The third term in Eq. (1) accounts for electrons leaving the distribution at ϵ as the result of ionization collisions. Although the two electrons produced by ionization are indistinguishable, we use the conventional terms of secondary and scattered primary to aid in bookkeeping. The relationships among these energies are illustrated in the energy map[18] shown in Fig. 1. Here the abscissa and ordinate are the energy u of the primary electron before ionization and the energies ϵ of the electrons produced by ionization. The secondary electrons are defined as the low-energy product electrons with energies below the dashed line. This line corresponds to an energy of $\epsilon=(u-u_i)/2$. Product electrons with energies between the dashed line and the solid line at $\epsilon=(u-u_i)$ are designated as scattered primary electrons or as scattered electrons. Note that the indistinguishability of the electrons and the conservation of energy leads to the requirement[3] that the distribution in energy ϵ of electrons produced by ionization be symmetrical about the energy $\epsilon=(u-u_i)/2$. The limits of integration in Eq. (1) can be recognized in Fig. 1 as the limits of the energies for secondary and scattered electrons for a fixed value of ϵ.

Four different forms of the secondary-electron energy distribution $q^i_{\text{sec}}(u,\epsilon)$ are considered in the present work. As the most realistic form, the differential ionization cross section determined from experiment by Opal, Peterson, and Beaty[2] is adopted. Thus

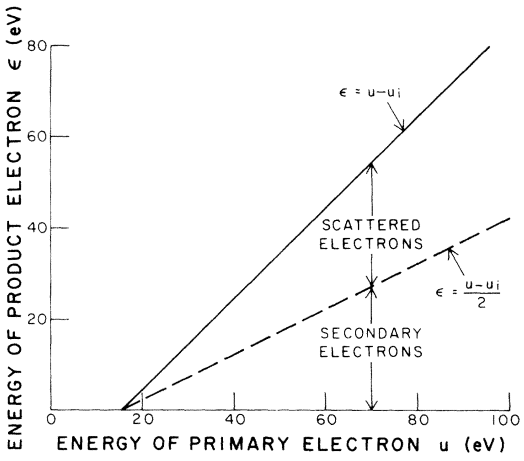

FIG. 1. Plot of energy of product electrons resulting from electron impact ionization of N_2 vs primary electron energy. Secondary electrons are defined as those below the dashed line, while scattered primary electrons are those between the dashed line and the solid line.

$$q^i_{\rm sec}(u,\epsilon)=\frac{Q_i(u)}{w\arctan\left[\dfrac{u-u_i}{2w}\right]}\,\frac{1}{1+\left[\dfrac{\epsilon}{w}\right]^2}\,, \tag{2}$$

where $Q_i(u)$ is the total ionization cross section and w is a constant determined experimentally. Because of the requirement of symmetry about $\epsilon=(u-u_i)/2$, the distribution in energy of the scattered electrons is related to the distribution for secondary electrons $q^i_{\rm sec}(u,\epsilon)$ by

$$q^i_{\rm sca}(u,\epsilon)=\frac{Q_i(u)}{w\arctan\left[\dfrac{u-u_i}{2w}\right]}\,\frac{1}{1+\left[\dfrac{u-u_i-\epsilon}{w}\right]^2}\,. \tag{3}$$

For each secondary-electron energy distribution considered the differential ionization cross section is related to the total ionization cross section by

$$Q_i(u)=\int_0^{(u-u_i)/2} q^i_{\rm sec}(u,\epsilon)d\epsilon\,. \tag{4}$$

It should be noted that in Eq. (4) $q^i_{\rm sec}(u,\epsilon)$ is integrated from 0 to $(u-u_i)/2$, rather than to $u-u_i$, so as to include only one of the product electrons.

Figure 2 shows plots of the distribution in energy of the product electrons given by Eqs. (2) and (3) versus normalized energy for the recommended value[2] of $w=13$ eV for N_2 and for primary-electron energies of 20, 50, and 200 eV. Note that by making w in Eq. (2) large compared to the largest value of $(u-u_i)/2$ encountered one can obtain an effectively uniform product-electron energy distribution.

In addition to the realistic case, calculations were performed for two extreme cases in order to see the effect of differences in the sharing of energy among the electrons produced by the ionization event. The two cases are the following.

(a) The ionization process in which a secondary electron appears with zero energy, i.e., along the horizontal axis of Fig. 1, and a scattered electron is produced with an energy equal to $u-u_i$, i.e., along the solid sloping line in Fig. 1. This differential cross section may be expressed in the form given by Thomas,[5] i.e., by Dirac δ functions $\delta(\epsilon)$ at $\epsilon=0$ and at $\epsilon=u-u_i$. In general, the δ-function approximation may be represented by

$$q^i_{\rm sec}(u,\epsilon)=Q_i(u)\delta(\epsilon-\tilde{\epsilon}) \tag{5a}$$

and

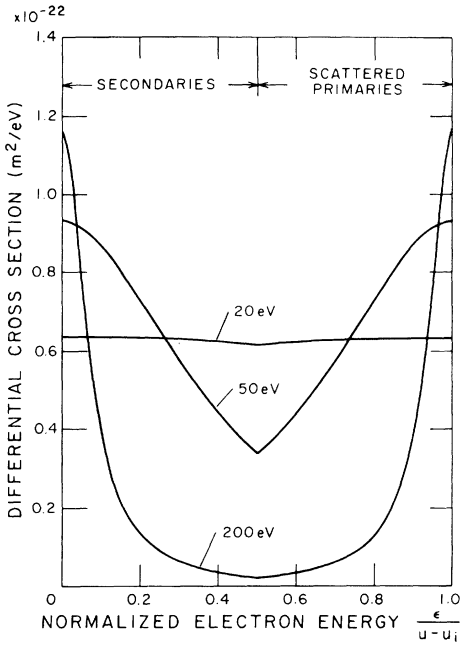

FIG. 2. Differential ionization cross sections vs normalized energy of the product electrons as calculated using the empirical approximation to experimental data from Opal, Peterson, and Beaty (Ref. 2) for primary energies of 20, 50, and 200 eV.

$$q^i_{\rm sca}(u,\epsilon)=Q_i(u)\delta[\epsilon-(u-u_i-\tilde{\epsilon})]\,, \tag{5b}$$

where $\tilde{\epsilon}$ is a function of $u-u_i$. However, in the present case $\tilde{\epsilon}=0$. Since this distribution minimizes the energy of the secondary electron, it also minimizes the energy loss by the scattered electron. This secondary-electron distribution is equivalent to that used in solutions of the Boltzmann equation[3,4] in which the secondary electron is accounted for by adjusting the flux of electrons entering the distribution at $\epsilon=0$ to equal the ionization frequency. The product-electron energy distribution given by Eqs. (5) can also be obtained by setting w in Eqs. (2) and (3) to a very small value, e.g., 0.1 eV in our calculations.

(b) The ionization process in which both electrons produced by ionization appear at the center of the available energy range, i.e., at the energy $\epsilon=(u-u_i)/2$ indicated by the sloping dashed line of Fig. 1. The differential ionization cross sections for this case may be expressed in the form of Eqs. (5) with

$$\tilde{\epsilon}=(u-u_i)/2\,. \tag{6}$$

This case gives the maximum available energy to the secondary electron and the largest possible energy loss to the scattered electron. The distribution given by Eq. (6) is that used in the multiterm calculations of ionization[15] in N_2 and is often identified as the distribution in which the product electron share equally the available energy.

Since the numerical solution of the Boltzmann equation, when formulated using Eqs. (2) and (3), required considerably longer computer time than when using Eqs. (5); we have developed an empirical product energy distribution utilizing δ functions which simulates the effects of the experimental product electron-energy distribution.[19] These distributions are obtained by using Eqs. (7) and (8) for $\tilde{\epsilon}$, i.e.,

$$\tilde{\epsilon}=\begin{cases}(u-u_i)/2 & \text{for } u<2\tilde{u}+u_i \quad (7)\\ \tilde{u} & \text{for } u>2\tilde{u}+u_i\,. \quad (8)\end{cases}$$

Here $\tilde{u}$ is an energy chosen to give the best fit to calculations using Eqs. (2) and (3). In Sec. III we will present the results of calculations using Eqs. (7) and (8) and a value of $\tilde{u}=13$ eV.

B. Boltzmann equation

The Boltzmann equation for an electron density which is spatially independent and exponentially increasing with time may be written in the two-term approximation[3,4,16] as

$$\frac{\epsilon}{vn}\frac{\partial f_0}{\partial t}+\frac{eE}{3n}\frac{\partial(\epsilon f_1)}{\partial\epsilon}=-\epsilon f_0(\epsilon)\sum_{k=1}Q_0^k(\epsilon)+\sum_{k=1}(\epsilon+u_k)Q_0^k(\epsilon+u_k)f_0(\epsilon+u_k)$$
$$+\frac{2m}{M}\frac{\partial}{\partial\epsilon}[\epsilon^2Q_m^0(\epsilon)f_0(\epsilon)]+\frac{\epsilon}{vn}\frac{\partial f_0(\epsilon)}{\partial t}\bigg|_{\text{ion}} \quad (9)$$

and

$$\frac{\epsilon}{vn}\frac{\partial f_1}{\partial t}+\frac{eE}{n}\epsilon\frac{\partial f_0}{\partial\epsilon}=-\epsilon f_1(\epsilon)\left[Q_m^0(\epsilon)+\sum_{k=1}Q_0^k(\epsilon)+Q_i(\epsilon)\right]=-\epsilon Q_m^e(\epsilon)f_1(\epsilon)\,, \quad (10)$$

where n is the gas density, M and m are masses of the gas molecule and of the electron, e is the electronic charge, $Q_m^0(\epsilon)$ is the elastic momentum transfer cross section ($k=0$), $Q_0^k(\epsilon)$ is the total excitation collision cross section for the kth excitation process, $Q_m^e(\epsilon)$ is an effective momentum transfer cross section, and $f_0(\epsilon)$ and $f_1(\epsilon)$ are the isotropic and the anisotropic or dipole components of the electron energy distribution function. Equations (9) and (10) also apply to the pulsed Townsend experiment,[12] i.e., to the spatially integrated solution of the Boltzmann equation. In Eq. (9) we have assumed that the mean electron energy is large enough so that terms proportional to the gas temperature[3] can be neglected. Note that in Eq. (10) we have neglected the excitation and ionization reentry terms, e.g., the terms of the form $(\epsilon+u_k)Q_1^k(\epsilon+u_k)f_1(\epsilon+u_k)$, where $Q_1^k(\epsilon)$ is the coefficient of the $P_1(\cos\theta)$ term of the spherical harmonic expansion of the differential cross section for the kth inelastic process. This approximation has been suggested by several authors[12,20] and is exact when the electron scattering during excitation and ionization is isotropic, e.g., when $Q_1^k(\epsilon)=0$. However, the electron scattering in N_2 is highly anisotropic at the higher energies of the present calculations,[15] so that the assumption is justified for slowly varying cross sections only when $f_1(\epsilon+u_k)$ is small compared to $f_1(\epsilon)$. Thus, when the $\partial f/\partial t$ terms are small we have retained the original form of the conventional two-term approximation[15] in which, as pointed out by Baraff and Buschbaum,[21] $Q_m^e(\epsilon)$ contains effects due to inelastic collisions.

We make the assumption that the number of electrons is increasing exponentially with time with a growth constant ν_i so that the time derivatives in Eqs. (9) and (10) are replaced by

$$\frac{\partial f_0(\epsilon)}{\partial t}=\nu_i f_0(\epsilon) \quad (11a)$$

and

$$\frac{\partial f_1}{\partial t}=\nu_i f_1(\epsilon)\,. \quad (11b)$$

Solving Eqs. (10) and (11) for $f_1(\epsilon)$, substituting into Eq. (9) and integrating from ϵ to $\epsilon=\infty$ yields the equation

$$\left[\frac{eE}{n}\right]^2\left[Q_m^e(\epsilon)+\frac{\nu_i}{vn}\right]^{-1}\left[\frac{\epsilon}{3}\right]\frac{df_0(\epsilon)}{d\epsilon}+\frac{2m}{M}\epsilon^2 Q_m(\epsilon)f_0(\epsilon)$$
$$=-\left[\frac{m}{2}\right]^{1/2}\left[\frac{\nu_i}{n}\right]\int_\epsilon^\infty u^{1/2}f_0(u)du-\sum_{k>0}\int_\epsilon^{\epsilon+u_k}uQ_0^k(u)f_0(u)du$$
$$+\int_{2\epsilon+u_i}^\infty uf_0(u)du\left[\int_\epsilon^{(u-u_i)/2}q_{\rm sec}^i(u,z)dz+\int_{(u-u_i)/2}^{u-u_i}q_{\rm sca}^i(u,z)dz\right]$$
$$+\int_{\epsilon+u_i}^{2\epsilon+u_i}uf_0(u)du\int_\epsilon^{u-u_i}q_{\rm sca}^i(u,z)dz-\int_\epsilon^\infty uQ_i(u)f_0(u)du\ . \tag{12}$$

Note that for the calculations reported in this paper the $2m/M$ term is negligible except at very low ϵ. Also note that, because of the use of the backward prolongation techniques[15] for finding $f_0(\epsilon)$, we have performed the integration leading to Eq. (12) from ϵ to ∞ rather than[1] from 0 to ϵ. The distribution function $f_0(\epsilon)$ is normalized by

$$\int_0^\infty \epsilon^{1/2}f_0(\epsilon)d\epsilon=1\ . \tag{13}$$

Except for the ionization terms, Eq. (12) is very similar to the Boltzmann equation solved[16] at low and moderate values of E/n. Note that the effects of growth of electron density described by Eqs. (11) are similar to those of a collision process which lowers the magnitude of the dipole component of the distribution and transfers energy between the "old" electrons and the new electrons so as to produce new electrons with the correct mean energy.[5] Equation (12) is solved numerically using the same techniques[16] as in the absence of ionization. Because of the presence of the unknown ν_i coefficient in Eq. (12), it is necessary to obtain $f_0(\epsilon)$ by iteration as discussed below.

In the case of a δ-function secondary-electron energy distribution, i.e., Eqs. (5), the ionization terms of Eq. (12) are given by

$$\int_\epsilon^\infty \frac{u}{vn}\left[\frac{\partial f_0(u)}{\partial t}\right]_{\rm ion}du$$
$$=\int_{u=x(\epsilon)+u_i}^\infty uQ_i(u)f_0(u)du$$
$$-\int_\epsilon^{u=y(\epsilon)+u_i}uQ_i(u)f_0(u)du\ . \tag{14}$$

Here $x(\epsilon)$ is equal to the value of $u-u_i$ for the desired ϵ as obtained from $\epsilon=\tilde{\epsilon}(u-u_i)$. Similarly, $y(\epsilon)$ is the value of $u-u_i$ at the ϵ obtained from $\epsilon=u-u_i-\tilde{\epsilon}(u-u_i)$. For the case considered by Thomas[5] of $\tilde{\epsilon}=\Delta(u-u_i)$, where Δ is a constant, $x(\epsilon)=\epsilon/\Delta$ and $y(\epsilon)=\epsilon(1-\Delta)^{-1}$. The shorter computer time required for the δ-function approximation is the result of the simpler integrals of Eq. (14) compared to those of Eq. (12).

Once $f_0(\epsilon)$ is obtained, the following transport coefficients and reaction coefficients can be calculated

$$k_i=\int_0^\infty vQ_i^0(\epsilon)f_0(\epsilon)d\epsilon\ , \tag{15}$$

$$\epsilon_k=\frac{E}{3W}\int_0^\infty\frac{v^2\epsilon^{1/2}f_0(\epsilon)d\epsilon}{vnQ_m^e(\epsilon)+\nu_i}\ , \tag{16}$$

$$W=-\frac{eE}{3}\int_0^\infty\frac{v^2\epsilon^{1/2}}{vnQ_m^e(\epsilon)+\nu_i}\frac{df_0(\epsilon)}{d\epsilon}d\epsilon\ , \tag{17}$$

$$\langle\epsilon\rangle=\int_0^\infty\epsilon^{3/2}f_0(\epsilon)d\epsilon\ , \tag{18}$$

where k_i is the ionization rate coefficient, W is the electron drift velocity, $\epsilon_k=D/\mu$ is characteristic energy,[16] and $\langle\epsilon\rangle$ is average electron energy. The iteration process used to obtain $f_0(\epsilon)$ requires that the input value of ν_i/n be adjusted until it is equal the value of k_i from Eq. (15). Often it is more satisfactory to obtain the correct value of ν_i by observing the convergence of the energy balance for the electrons.[15] Note that Eqs. (16) and (17) differ from the conventional expressions[3,4] for ϵ_k and W because of the inclusion of ν_i in the denominator of the integrands.

III. RESULTS AND DISCUSSION

The results of this investigation are seen from examination of the isotropic component of the electron-energy distribution $f_0(\epsilon)$, the ionization rate coefficient ν_i/n, the transport coefficients W and ϵ_k, and the mean electron energy $\langle\epsilon\rangle$. Most of the calculations were carried out for an E/n of 1500×10^{-21} V m^2, for which the effects of changes in the secondary distribution are large and for which the two-term approximation yields values in reasonable agreement with more detailed calculations.

Figures 3–5 show calculated electron-energy distributions for the various secondary-electron energy distributions discussed in Sec. II A. The various curves are labeled A through H and the conditions for which they were calculated are listed in Table I. Table I also lists the ionization and transport coefficients calculated from the distribution functions. The last column of Table I shows the large fraction of the input energy required to produce the new electron and the positive ion.

A. Fixed E/n

The electron-energy distribution calculated when the reentry of secondary electrons is omitted from the Boltzmann equation, i.e., when $q^i_{\rm sec}(u,\epsilon)=0$ and ionization is treated as an excitation process, is shown by curve A of Figs. 3 and 4. In this calculation and in the calculations for curves B–E, we assume $\nu_i f_1(\epsilon)=0$ in Eq. (11b) and neglect ν_i in the left-hand side of Eq. (12) and in Eqs. (16) and (17), so that the assumptions are the same as for most previous calculations for N_2.[12,22] Note that these assumptions are not made in some of the more detailed recent N_2 calculations[15,23] and in cases G and H discussed below. When the secondary electrons are included, the relative number of very-low-energy electrons $\epsilon < 10$ eV is significantly increased as shown by comparison of curves B, C, and E with curve A in Fig. 3. Curve B shows the electron-energy distribution obtained when the secondary electrons reenter the distribution with essentially zero energy, e.g., $w=0.1$ eV in Eq. (3). The same distribution is obtained when ionization is treated like excitation in Eqs. (1) and the normalized growth constant ν_i/n in Eq. (11a) is adjusted to equal the ionization rate coefficient k_i, i.e., when Eqs. (5) are used with $\tilde{\epsilon}=0$. In this case the flux of reentering electrons determines the strength of the integrable singularity[3,4] in $f_0(\epsilon)$ at $\epsilon=0$.

Curves B, C, D, and E in Figs. 3 and 4 show the effects of progressively increasing the mean energy of the secondary electrons and, as required by energy conservation, of increasing the energy lost by the scattered electrons. As the mean energy of the secondary electrons increases in going from curve B to curve E there is a decrease in the number of very-low-energy electrons. In addition, the high-energy portions of the calculated distribution functions also decrease as the scattered electron loses more energy. Thus, the maximum possible energy

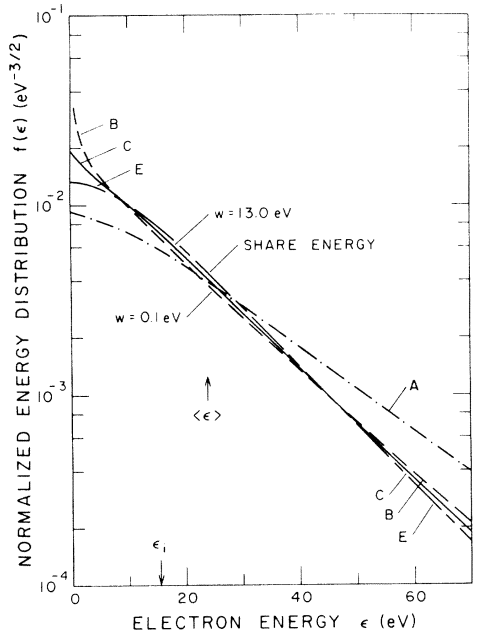

FIG. 3. Normalized electron-energy distributions calculated for $E/n=1500\times10^{-21}$ V m^2 and various representative distributions in energy of secondary electrons. Curve A is calculated neglecting the secondary electron. Curves B and C are for values of the width parameter w of 0.1 and 13 eV, respectively. Curve E is calculated assuming that the product electrons share the available energy equally. See Table I for further data for these cases.

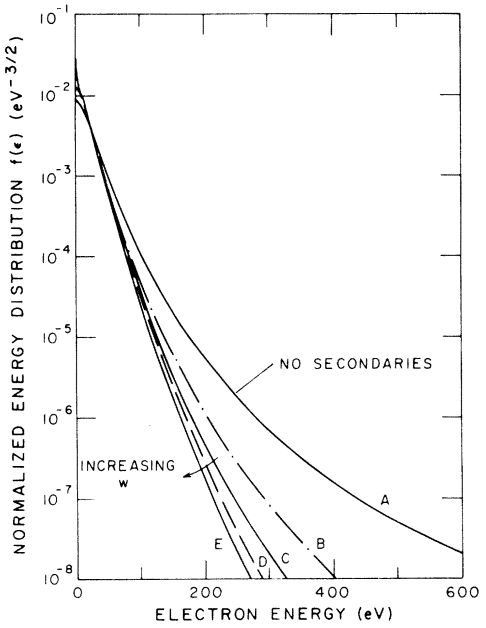

FIG. 4. Normalized electron-energy distributions calculated for various distributions in energy of the scattered primary electrons. Curves are those of Fig. 1 and are identified in Table I. $E/n=1500\times10^{-21}$ V m^2.

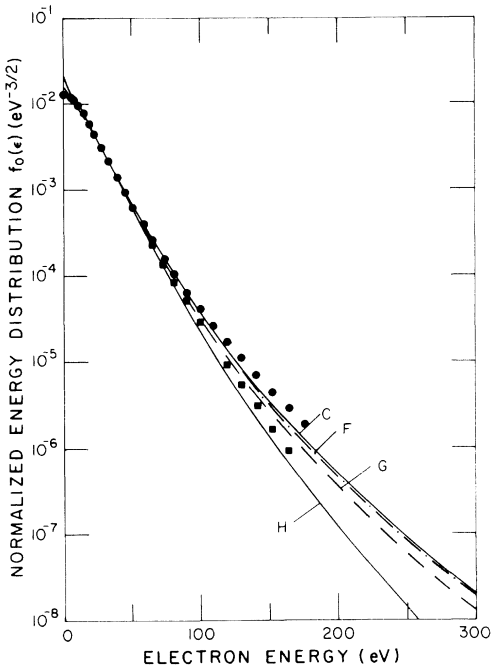

FIG. 5. Comparison of normalized electron-energy distributions calculated using experimental distribution (curve C), empirical δ-function approximation (curve F), and including the ionization frequency in the $f_1(\epsilon)$ equation (curves G and H). Squares show the effects of anisotropic inelastic collisions in the two-term approximation, while the circles show the six-term results with anisotropic scattering. $E/n = 1500\times10^{-21}$ V m^2.

loss for the scattered electron and the smallest relative number of high-energy electrons occur when the two product electrons share the available energy, i.e., when $\epsilon=(u-u_i)/2$ as for curve E. Also of interest is the change in slope of the energy distributions of Fig. 4 which occurs at electron energies from 100 to 200 eV. At energies above this range the cross sections for energy loss decrease with increasing energy and the electrons tend to undergo runaway,[24] particularly when the energy loss to ionization by the scattered electrons is small as for curve B. Because of the incipient runaway effects shown by experimental Townsend ionization coefficient measurements[25] for N_2, we have limited our calculations to $E/n \leq 3000\times10^{-21}$ V m^2.

Curve F of Fig. 5 and the corresponding entries in Table I show the results of calculations using the empirically adjusted δ function approximation to the product electron-energy distribution given in Eqs. (7) and (8). In this case the reaction and transport coefficients are within 5% of those calculated with the Opal, Peterson, and Beaty distribution and shown by curve C. The other electron-energy distributions of Fig. 5 show the effects of refinements in the Boltzmann equation used for the calculations. Thus, curves G and H show the effect of including the exponential growth of the electron distribution as represented by ν_i in Eq. (10) for the dipole component of the energy distribution $f_1(\epsilon)$ and are to be compared with curves C and E, respectively. Curve G and the corresponding transport coefficients in Table I are the most accurate of the results obtained with the two-term approximations presented in this paper. A comparison of the entries for curves C and G and for curves E and H in Table I shows changes in the ionization and transport coefficients of less than 10% with the largest changes occurring in the drift velocities, i.e., in coefficients where ν_i enters directly into the calculation through Eqs. (16) and (17). The relative changes in $f_0(\epsilon)$ caused by

TABLE I. Calculated ionization and transport coefficients for electrons in N_2 at $E/n = 1500\times10^{-21}$ V m^2.

Case	$q^i_{\rm sec}(u,\epsilon)$	w (eV)	k_i (m^3/sec)	W (m/sec)	ϵ_k (eV)	$\langle\epsilon\rangle$ (eV)	Percentage energy to ionization[b]
A	None		4.01(−14)[a]	8.40(5)	22.9	34.1	75.7
B	$\tilde{\epsilon}=0$, Eqs. (2) and (3)	0.1	2.44(−14)	9.52(5)	15.2	23.8	66.9
C	Eqs. (2) and (3)	13	2.33(−14)	9.17(5)	15.5	23.2	65.3
D	Eqs. (2) and (3)	500	2.28(−14)	9.10(5)	15.6	23.1	64.6
E	Eq. (6)		2.22(−14)	8.94(5)	15.8	23.0	63.7
F	Eqs. (7) and (8)	$\tilde{u}=13$	2.24(−14)	9.00(5)	15.8	23.1	64.3
G[c]	Eqs. (2) and (3)	13	2.17(−14)	8.56(5)	15.0	22.4	63.9
H[c]	Eq. (6)		2.09(−14)	8.41(5)	15.2	22.2	62.5

[a]4.01(−14) means 4.01×10^{-14}.

[b]This is equal to $100(\nu_i/n)(\epsilon_i+\langle\epsilon\rangle)(WeE/n)^{-1}$. See, for example, Eq. (12) of Ref. 5.

[c]Note that the ν_i term was included in Eqs. (10), (16), and (17) for these cases.

changes in $q^i_{sec}(u,\epsilon)$ are nearly the same when ν_i is included in Eq. (10) as the changes shown in Figs. 3 and 4 for calculations when ν_i is omitted.

We now compare the electron-energy distribution and associated transport coefficients obtained using the present techniques with the results obtained using the techniques for solution of the Boltzmann equation which are described in Ref. 17 for N_2. The electron-energy distribution $f_0(\epsilon)$ calculated using the latter techniques for the conditions of curve H of Fig. 5, i.e., for an equal sharing of energy by the product electrons, the inclusion of the time derivative in the dipole equation and treating inelastic scattering as isotropic in a two-term spherical harmonic approximation, is virtually indistinguishable from curve H for the range of the calculations ($\epsilon < 170$ eV). Good agreement between the two procedures is also obtained for the conditions of curve E of Fig. 4. The transport coefficients in both cases differ by 3% or less from those listed in Table I. These comparisons show the consistency of the present calculational procedure with that of Ref. 17 and show the usefulness of the effective momentum transfer cross section defined by Eq. (10) when the electron scattering is isotropic.

Finally, we briefly consider the effects of anisotropic electron scattering. Thus, the solid squares and circles of Fig. 5 show the results of calculations of $f_0(\epsilon)$ in which the complete set of anisotropic scattering cross sections of Ref. 15 were used for two-term and six-term calculations. In particular, the differences between the squares and curve H show the errors resulting from the approximation of Eq. (10) in which the terms involving the asymmetric components of the inelastic cross sections, e.g., the $Q^k_1(\epsilon)$, are neglected. The ionization coefficient and drift velocity are 8% higher and the characteristic energy is 3% lower for the anisotropic scattering calculation than for curve H. The higher drift velocity results from the reduction in the contribution of collisions to the multiterm version of Eq. (10) at energies above about the mean electron energy. Similarly, the larger ionization coefficient results from the larger $f_0(\epsilon)$ for $\epsilon > \langle\epsilon\rangle$. The differences between the circles and the squares show the effect on $f_0(\epsilon)$ of changing from a two-term solution to a six-term solution,[17] e.g., the results show the expected[15] 20% decrease in the slope of $f_0(\epsilon)$ when the larger number of spherical harmonics is used. On the other hand, the ionization coefficient, drift velocity, and mean electron change by less than 0.5% from the two-term, anisotropic scattering results. This unexpectedly small change in the ionization coefficient is the result of the changes in $f_0(\epsilon)$ due to changes in slope and renormalization, i.e., a decrease in ionization by electrons with $\epsilon < 50$ eV and an increase in ionization by electrons with $\epsilon > 50$ eV. A similar cancellation of changes occurs for the other coefficients.

We conclude that when the same secondary-electron energy distribution and angular scattering distribution is used in both calculations, the ionization coefficient, drift velocity, and mean electron energy are reasonably accurately given by the two-term approximation described in this paper. However, accurate calculations of the high-energy portion of $f_0(\epsilon)$ and of ϵ_k require the multiterm solutions. It will be recalled[17] that the situation is similar at low E/n in N_2, where the errors in the calculated distribution function at the higher electron energies and in the excitation coefficients can be large. The relation between two-term and higher multiterm solutions with isotropic and anisotropic scattering at high E/n is considered in more detail elsewhere.[15]

B. Variable E/n

The calculations discussed in the preceding paragraphs for 1500×10^{-21} V m^2 have also been carried out for 100×10^{-21} V m$^2 \leq E/n \leq 3000\times10^{-21}$ V m^2 and for several of the secondary-electron distributions listed in Table I. Figures 6 and 7 show the calculated values of the ionization coefficient, the electron drift velocity, and the characteristic energy ϵ_k for the cases in which the secondary electron was neglected (curves A); in which the secondary electron was given zero energy (curves B); and the experimental distribution in energy of Eqs. (2) and (3) (curves C). These results show that the effects of secondary electrons on all three coefficients are negligible for $E/n < 300\times10^{-21}$ V m^2, as assumed by Engelhardt, Phelps, and Risk.[22] The calculated ionization coefficients in Fig. 6 are only moderately sensitive to the detailed form of the secondary-electron energy distribution provided the secondaries are included. Note that these calculated k_i values are significantly higher than the values calculated from the measurements of the spatial growth of electron current by Folkhard and Haydon[25] which are shown by the points in Fig. 6. According to the calculations of Taniguchi, Tagashira, and Sakai[23] for N_2 this difference is approximately that expected between calculations which take into account the temporal growth of the electron density and calculations which take into account the spatial growth of electron density.

The changes in electron drift velocity with changes in secondary-electron energy distribution shown in Fig. 7 are small. Also, the agreement with the experimental values[26–28] is reasonably good.

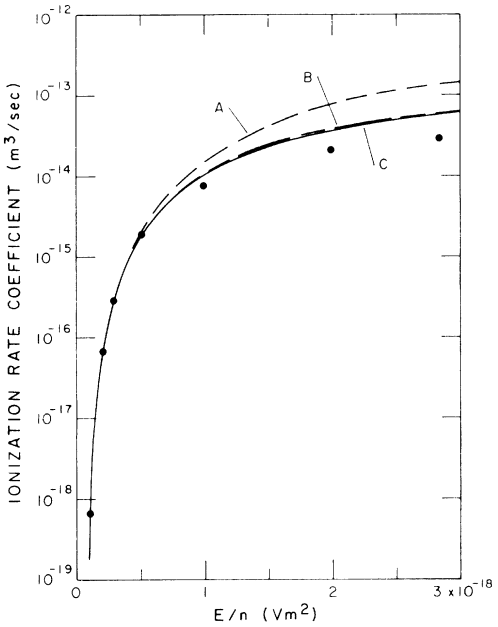

FIG. 6. Ionization coefficients for N_2 calculated using various approximations for the distribution in energy of the secondary electrons (curves A—C). Experimental data from Ref. 24 are shown by the points for comparison with theory.

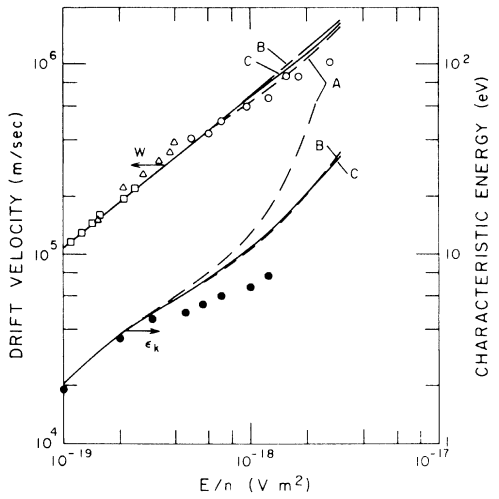

FIG. 7. Electron drift velocities and characteristic energies calculated using various approximations to the distribution in energy of secondary electrons. The points are the results of experiment, i.e., □, Ref. 26; △, Ref. 27; ○, Ref. 28; ●, Ref. 29.

The calculated values of the characteristic energy are very sensitive to whether or not the secondary electron is included in the Boltzmann equation but are relatively insensitive to the details of the distribution in energy of the secondary electron. We note that the average electron energies in Table I show much the same change with the assumed secondary-electron distribution as do the characteristic energies. Both of these energies rise very rapidly with E/n at high E/n, as expected when the runaway condition is approached[25] at E/n near 3400×10^{-21} V m^2. As shown in Fig. 7, the calculated values of the characteristic energy at E/n values above 400×10^{-21} V m^2 are much larger than the experimental data taken from Kontolen, Lucas, and Virr.[29] As mentioned above, the calculated values of ϵ_k are expected to be somewhat in error because of the failure of the calculations shown in Fig. 7 to take into account density gradients.[17,23] However, the characteristic energy calculated at $E/n=1500\times10^{-21}$ V m^2 using the multiterm spherical harmonic technique[17] is also significantly larger than the experimental data.

IV. SUMMARY

The calculations of electron-energy distributions and of ionization and transport coefficients presented in this paper confirm previous conclusions that it is necessary to include the effects of the production of new electrons by collisional ionization. In addition, we found that the number of very-low-energy and of high-energy electrons is a sensitive function of the distribution in energy of the scattered and secondary electrons. While the calculated ionization and transport coefficients are less sensitive functions of the secondary-electron distribution, accurate calculations require a reasonably accurate representation of the secondary distribution. In order to simplify the numerical calculations we have developed an empirical δ-function representation of the distribution in energy of the product electrons which yields solutions to the electron Boltzmann equation and transport coefficients which are in good agreement with calculations based on the experimental secondary-electron distributions. Now that simple and reasonably accurate representations of the effects of realistic secondary and scattered electron-energy distributions have been found for gases such as N_2, we can concentrate our efforts to obtain reliable solutions of the electron Boltzmann equation at high E/n on problems such as the high degree of anisotropy of the distribution function at high-electron energies.

ACKNOWLEDGMENTS

We would like to acknowledge the help of C. V. Kunasz in the modifications of the computer programs used in this work. The work of S. Y. and A. V. P. was supported in part by the U. S. Army Research Office, while that of L. C. P. was supported by the U. S. Department of Energy.

*Present Address: Department of Electrical Engineering, Keio University, Yokahama 223, Japan.
†Quantum Physics Division, National Bureau of Standards and Department of Physics, University of Colorado.

[1]H. Brunet and P. Vincent, J. Appl. Phys. 50, 4700 (1979); 4708 (1979). There appear to be several errors in Eq. (7) of the first of these references.
[2]C. B. Opal, W. K. Peterson, and E. C. Beaty, J. Chem. Phys. 55, 4100 (1971).
[3]T. Holstein, Phys. Rev. 70, 367 (1946).
[4]W. P. Allis, *Handbuch der Physik,* edited by S. Flugge (Springer, Berlin, 1956), Vol. 21, p. 383.
[5]W. R. L. Thomas, J. Phys. B 2, 551 (1969).
[6]A. A. Garamoon and I. A. Ismail, J. Phys. D 10, 991 (1977); 105 (1977).
[7]Y. Sakai, H. Tagashira, and S. Sakamoto, J. Phys. D 10, 1035 (1977); 1051 (1977).
[8]J. Wilhelm and R. Winkler, Ann. Phys. (Leipzig) 36, 333 (1979); 352 (1979).
[9]C. H. Chan and C. D. Moody, J. Appl. Phys. 45, 1105 (1974).
[10]E. E. Kunhardt and Y. Tzeng, in Proceedings of the Second Gaseous Electronics Meeting, Haydon, edited by S. C. Armidale, Australia, February, 1982 (unpublished).
[11]H. Schulbohm, Z. Phys. 184, 492 (1965); J. Wilhelm and R. Winkler, Ann. Phys. (Leipzig) 23, 28 (1969).
[12]R. Winkler and S. Pfau, Beitr. Plasmaphys. 13, 273 (1973); 14, 169 (1974).
[13]L. Ferrari, Physica 81A, 276 (1975); 85C, 161 (1977); J. H. Jacob, B. N. Srivastava, M. Rokni, and J. A. Mangano, J. Appl. Phys. 50, 3185 (1979); S. L. Lin, R. E. Robson, and E. A. Mason, J. Chem. Phys. 71, 3483 (1979); T. Makabe and T. Mori, J. Phys. D 13, 387 (1980); W. P. Allis, Phys. Rev. A 26, 1704 (1982).
[14]K. Kumar and R. E. Robson, Aust. J. Phys. 26, 157 (1973); K. Kitamori, H. Tagashira, and Y. Sakai, J. Phys. D 11, 283 (1978).
[15]L. C. Pitchford and A. V. Phelps, Bull. Am. Phys. Soc. 27, 109 (1982).
[16]L. S. Frost and A. V. Phelps, Phys. Rev. 127, 1621 (1962). For details of this computer program see P. H. Luft, Joint Institute for Laboratory Astrophysics Information Center Report No. 14, University of Colorado, 1975 (unpublished).
[17]L. C. Pitchford and A. V. Phelps, Phys. Rev. A 25, 540 (1982). See also, L. C. Pitchford, S. V. O'Neil, and J. R. Rumble, Jr., *ibid.* 23, 294 (1981).
[18]J. Bretagne, G. Delouya, J. Godart, and V. Puech, J. Phys. D 14, 1225 (1981).
[19]A potentially more useful and accurate empirical expression for $\tilde{\epsilon}$ for use in Eqs. (5) is to assume that $\tilde{\epsilon}=(2w/\pi)\ln[1+(u-u_i)/2w]$ instead of the values given in Eqs. (7) and (8). This expression is chosen to give secondary electrons with an energy which is equal to the mean energy calculated from Eq. (2) to within 10% for $(u-u_i)/w>0.2$.
[20]I. Abdelnabi and H. S. W. Massey, Proc. Phys. Soc. London 66, 288 (1953); J. L. Losee and D. S. Burch, Phys. Rev. A 6, 1652 (1972); W. H. Long, Jr. and W. F. Bailey, Bull. Am. Phys. Soc. 19, 151 (1974).
[21]G. A. Baraff and S. J. Buchsbaum, Phys. Rev. 130, 1007 (1963).
[22]A. G. Engelhardt, A. V. Phelps, and C. G. Risk, Phys. Rev. 135, A1566 (1964); L. A. Newman and T. A. DeTemple, J. Appl. Phys. 47, 1912 (1976); A. Kh. Mnatsakanyan and G. V. Naidis, Fiz. Plasmy 2, 152 (1976) [Sov. J. Plasma Phys. 2, 84 (1976)]; K. Rohlena and T. Ruzicka, Czech. J. Phys. B 29, 407 (1979); N. L. Aleksandrov, A. M. Konchakov, and É. E. Son, Teplofiz. Vys. Temp. 17, 210 (1979) [High Temp. (USSR) 17, 179 (1979)]; M. Capitelli, M. Dilonardo, and C. Gorse, Chem. Phys. 56, 29 (1981).
[23]T. Taniguchi, H. Tagashira, and Y. Sakai, J. Phys. D 11, 1757 (1978).
[24]A. V. Gurevich, Zh. Eksp. Teor. Fiz. 39, 1296 (1960) [Sov. Phys.—JETP 12, 904 (1961)]; G. Ecker and K. G. Muller, Z. Naturforsch. 16a, 246 (1961).
[25]M. A. Folkhard and S. C. Haydon, Aust. J. Phys. 24, 519 (1971); J. Phys. B 6, 214 (1973).
[26]L. Fromhold, Z. Phys. 120, 540 (1960).
[27]K. H. Wagner and H. Rather, Z. Phys. 170, 540 (1962); K. H. Wagner, *ibid.* 178, 64 (1964).
[28]H. Schulmbohm, Z. Phys. 182, 317 (1965).
[29]N. Kontoleon, J. Lucas, and L. E. Virr. J. Phys. D 6, 1237 (1973).